Dissociative electron attachment and electron-impact resonant dissociation of vibrationally excited O2 molecules

Dissociative electron attachment and electron-impact resonant dissociation of vibrationally excited O_2 molecules

V. Laporta,[1,2,*] R. Celiberto,[3,1] and J. Tennyson[2]

[1] *Istituto di Metodologie Inorganiche e dei Plasmi, CNR, Bari, Italy*
[2] *Department of Physics and Astronomy, University College London, London WC1E 6BT, UK*
[3] *Dipartimento di Ingegneria Civile, Ambientale, del Territorio, Edile e di Chimica, Politecnico di Bari, Italy*

State-by-state cross sections for dissociative electron attachment and electron-impact dissociation for molecular oxygen are computed using *ab initio* resonance curves calculated with the R-matrix method. When O_2 is in its vibrational ground state, the main contribution for both processes comes from the $^2\Pi_u$ resonance state of O_2^- but with a significant contribution from the $^4\Sigma_u^-$ resonant state. Vibrational excitation leads to an increased contribution from the low-lying $^2\Pi_g$ resonance, greatly increased cross sections for both processes and the threshold moving to lower energies. These results provide important input for models of O_2-containing plasmas in non-equilibrium conditions.

PACS numbers: 34.80.Ht, 34.80.Gs, 52.20.Fs

I. INTRODUCTION

Molecular oxygen is a major component of the Earth's atmosphere and is fundamental for life. It plays an important role in many natural and technological processes. In this paper we focus on the ability of low-energy electrons to dissociate molecular oxygen, in its fundamental electronic state, by means of resonant scattering. In particular we consider the state-by-state processes of dissociative electron attachment (DEA),

$$e^- + \mathrm{O}_2(\mathrm{X}\,^3\Sigma_g^-; v) \rightarrow \mathrm{O}_2^{-*} \rightarrow \mathrm{O}^-(^2\mathrm{P}) + \mathrm{O}(^3\mathrm{P})\,, \quad (1)$$

and electron impact dissociation (EID),

$$e^- + \mathrm{O}_2(\mathrm{X}\,^3\Sigma_g^-; v) \rightarrow \mathrm{O}_2^{-*} \rightarrow e^- + 2\,\mathrm{O}(^3\mathrm{P})\,, \quad (2)$$

for each oxygen vibrational level v. The threshold for the process (1) is 3.64 eV, corresponding to the asymptotic energy of O and O^- fragments from the level $v = 0$, whereas for process (2) corresponds to the oxygen dissociation of 5.11 eV.

Such collisions are important to study phenomena occurring in the upper atmosphere, re-entry physics, electrical discharges and plasma chemistry. DEA is the principal mechanisms, in molecular plasmas, for forming negative ions from neutral molecules; the inverse process represents associative detachment. Although significant theoretical and experimental effort has been invested in characterizing electron-O_2 cross sections [1], information is only available for the vibrational ground state of O_2 for which both processes have rather small cross sections. Here, we will show that DEA and EID processes become much more important for vibrationally excited oxygen, as the corresponding cross sections increases by orders of magnitude with the excitation of the molecule. These cross sections represent fundamental input quantities in kinetics models of oxygen-containing non-equilibrium plasmas, where high-lying vibrational levels of molecules can be hugely populated.

The paper is organized as follow: In the Section II we will give a brief account and numerical details on the adopted theoretical models for the calculation of the potential energy curves and on the description of the nuclear dynamics. The results are illustrated in Section III while the concluding remarks are given in Section IV.

II. THEORETICAL MODEL

Many low-energy electron-molecule scattering processes are dominated by resonances. For molecular oxygen these processes can be quantitatively understood in term of four low-lying O_2^- resonances of symmetry $^2\Pi_g$, $^2\Pi_u$, $^4\Sigma_u^-$ and $^2\Sigma_u^-$. First calculations were made by Noble *et al.* [2] who used the R-matrix method [3] to determine the positions and widths for these four resonances. The O_2 target was represented using nine states, corresponding to the orbital configurations: $[core]1\pi_u^4 1\pi_g^2$ and $[core]1\pi_u^3 1\pi_g^3$. The scattering T-matrix was calculated, in the fixed-nuclei approximation, for internuclear distance range $[1.85, 3.5]\,a_0$, using the configurations: $[core]1\pi_u^4 1\pi_g^3\,(^2\Pi_g)$, $[core]1\pi_u^3 1\pi_g^4\,(^2\Pi_u)$, $[core]1\pi_u^4 1\pi_g^2 3\sigma_u\,(^4\Sigma_u^-)$ and $[core]1\pi_u^4 1\pi_g^2 3\sigma_u\,(^2\Sigma_u^-)$, for energies up to 15 eV.

In our previous paper on state-to-state cross sections for resonant vibrational excitation (RVE) for electron-oxygen scattering [4], we extended Noble *et al.*'s calculations toward larger internuclear distances using the quantum chemistry code MOLPRO [5]. We used a multi-reference configuration interaction (MRCI) model and an aug-cc-pVQZ basis set. For the neutral ground-state of O_2 as well as for the real part of its anionic state O_2^-, the active space included the first 2 core orbitals ($1\sigma_g$,$2\sigma_g$) and 8 valence orbitals ($2\sigma_g$, $3\sigma_g$, $2\sigma_u$,$3\sigma_u$, $1\pi_u$, $1\pi_g$) plus 150 external orbitals for a total of 160 contractions. The MRCI orbitals were taken from a ground-state multi-

*Electronic address: vincenzo.laporta@imip.cnr.it

configuration self-consistent field (MCSCF) calculation in which 4 electrons were kept frozen in the core orbitals and excitations among all the valence orbitals were considered for the 12- and 13-electrons of the neutral and ionic state respectively.

In the present work we update Noble *et al.*'s R-matrix calculations in order to have a better representation of the states involved in the scattering processes. Calculations were performed using the UKRMol codes [6]. Orbitals for the O_2 were generated using configuration interaction (CI) calculations using a cc-pVTZ Gaussian-type orbital (GTO) basis set. The electrons in the lowest 3 core orbitals, $(1\sigma_g,2\sigma_g,1\sigma_u)^6$, were frozen and an active space was constructed from 9 valence orbitals $(3\sigma_g,$ $2\sigma_u,3\sigma_u,$ $1\pi_u,$ $2\pi_u,$ $1\pi_g)^{10}$. The scattering calculations with 17 electrons also used a GTO basis [7] to represent the continuum electron. The calculations were based on use of a complete active space CI representation which involves placing the extra electron in both a continuum orbital and target orbitals using the following prescription: $(1\sigma_g,2\sigma_g,$ $1\sigma_u)^6$ $(3\sigma_g,$ $2\sigma_u,3\sigma_u,$ $1\pi_u,$ $2\pi_u,$ $1\pi_g)^{11}$ and $(1\sigma_g,2\sigma_g,$ $1\sigma_u)^6$ $(3\sigma_g,$ $2\sigma_u,3\sigma_u,$ $1\pi_u,$ $2\pi_u,$ $1\pi_g)^{10}$ $(4\sigma_g,$ $5\sigma_g,$ $3\pi_u,$ $4\sigma_u,$ $2\pi_g,$ $3\pi_g,$ $1\delta_g,$ $1\delta_u)^1$, where the second set of configurations involves placing the extra electron in an uncontracted [8] target virtual orbital. Calculations used an R-matrix radius of 10 a_0. Both the MOLPRO and R-matrix calculations were performed using D_{2h} symmetry.

The potential curves calculated with the R-matrix and MOLPRO codes use different basis-sets, different theoretical models and computational methods. This means that the resulting curves did not join and a merging procedure was required. First of all the O_2 neutral ground-state potential was calculated using MOLPRO and all the subsequent results were referred to this curve. The real part of the resonance potentials, computed as a bound scattering state in the R-matrix calculations, was fixed at large internuclear distances beyond the crossing point to the MOLPRO curve which precisely reproduces the experimental oxygen atom electron affinity of 1.46 eV. At shorter internuclear distances, the R-matrix resonant curves, are simply a smooth continuation of these large R curves and therefore their positions are fixed by the corresponding MOLPRO curve. Potential energy curves for the $O_2(X\,^3\Sigma_g^-)$ ground state, which supports 42 vibrational states, and the four resonance states, plus the corresponding widths, are reported in Fig. 1. We note that the new calculated potentials are slightly changed with respect to those of our previous paper [4], in particular for the $^2\Pi_u$ symmetry, and this could affect the RVE cross section values. To check this aspect, we performed new calculations for RVE processes, observing however no significant changes in the cross sections with respect to the corresponding results in [4].

Previously [4] we showed that for energies up to about 4 eV the RVE cross sections are characterized by narrow spikes dominated by the $^2\Pi_g$ resonance. For energies about 10 eV, the cross sections showed a broad maximum due to enhancement by the $^4\Sigma_u^-$ resonance with a

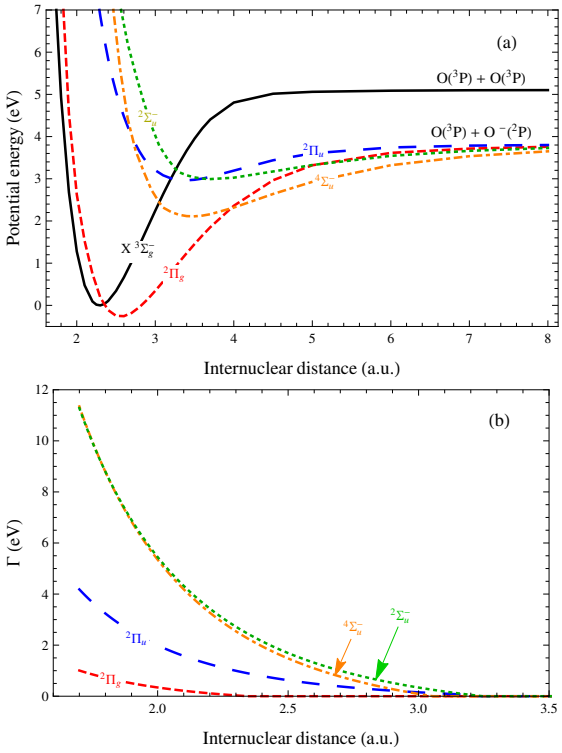

FIG. 1: (Color online) (a) Potential energy curves for ground state $X\,^3\Sigma_g^-$ of O_2 and for the four lowest resonant states O_2^-; (b) The corresponding resonance widths, $\Gamma(R)$, as a function of the internuclear distance.

smaller contribution coming from the $^2\Sigma_u^-$ state. In the case of DEA and EID processes we show that they are dominated, at least for low vibrational levels v of O_2, by the $^2\Pi_u$ resonance. Although electron attachment from oxygen molecules has been widely studied [9] there are only a few, rather old, papers reporting cross section measurements of the DEA process as a function of the incident electron energy. We cite here Rapp and Briglia [10], Schulz [11] and Christophorou *et al.* [12]. DEA from the $^1\Delta_g$ state of O_2 has also been observed [13] and found to have a cross section of similar magnitude to process (1). Cross sections for EID only appear to have been measured for electronically excited states of O_2 by Cosby [14].

In Born-Oppenheimer approximation, the dynamics of the oxygen nuclei in DEA is treated within the local-complex-potential model [15], already satisfactory adopted for resonant calculations in other diatomic molecules (see Refs. [4, 16] and references therein). The corresponding cross section from the vibrational level v of oxygen and for electron energy ϵ is given by:

$$\sigma_v(\epsilon) = 2\pi^2 \frac{m_e}{k} \frac{K}{\mu} \lim_{R\to\infty} |\xi(R)|^2 \,, \qquad (3)$$

where K is the asymptotic momentum of the dissociating fragments O and O^- with reduced mass μ; m_e and $k = \sqrt{2m_e\epsilon}$ are the incoming electron mass and momentum respectively and $\xi(R)$ is the solution of the Schrodinger-

like equation for the resonant state and total energy $E = \epsilon_v + \epsilon$:

$$\left(-\frac{\hbar^2}{2\mu}\frac{d^2}{dR^2} + V^- + \frac{i}{2}\Gamma - E\right)\xi(R) = -V\,\chi_v(R)\,, \quad (4)$$

where $V^- + \frac{i}{2}\Gamma$ is the complex potential of the resonance reported in Fig. 1, $V^2 = \Gamma/(2\pi\,k)$ is the discrete-to-continuum potential coupling and χ_v is the vibrational wave function of O_2 corresponding to the vibrational level v. R represents the internuclear distance. There is not interference among the resonant states with different symmetries and for the two Σ_u^- states the interference can be considered negligible as they have different spin multiplicity.

III. RESULTS AND DISCUSSION

Figure 2(a) shows our results for the DEA cross section for $O_2(v = 0)$ compared with the experimental results of Rapp and Briglia [10], Schulz [11] and Christophorou *et al.* [12]. The agreement is excellent, within the experimental error of ±15%: the peak is positioned at 6.43 eV with an absolute value of 0.0154 Å^2 and the FWHM of about 2 eV. Fig. 2(b) reports cross sections coming from all four resonances and their sum. As found experimentally, the main contribution to DEA cross section comes from the $^2\Pi_u$ state of O_2^-. We also note, at about 8.5 eV, the presence of a significant contribution due to the $^4\Sigma_u^-$ symmetry which, added to the main $^2\Pi_u$ contribution, reproduces the high-energy tail observed experimentally. The non-negligible contribution of $^4\Sigma_u^-$ resonance to DEA cross section has already been deduced from the measured angular distribution of O^- ions [17].

Figure 3 shows our DEA cross sections calculated for higher vibrational levels of O_2, $v = 10, 20$ and 30, compared with the result $v = 0$. All cross sections are summed over all four resonance states. As expected [18], the threshold of the process shifts to lower energies as the vibrational level increases; the is due to the reduced threshold for dissociation limit. At same time the maximum value of the cross section for $v < 30$ grows by of several orders of magnitude at low energies. This behaviour is due to the survival factor $e^{-\rho}$ [19], given approximatively by:

$$e^{-\rho} \simeq \exp\left[-\int_{R_e}^{R_c}\frac{\Gamma(R)dR}{\hbar v(R)}\right]\,, \quad (5)$$

where integration is extended over the region between the classical turning point (R_e) and the stabilization point (R_c) and $v(R)$ is the classical velocity of dissociation. As the vibrational level increases, R_e increases and the survival probability grows like the cross section. The oscillations, visible at high vibrational levels, results from the interplay between the neutral vibrational wave function and the resonant continuum wave function. Analysis of the resonance contributions to the cross section at $v = 20$

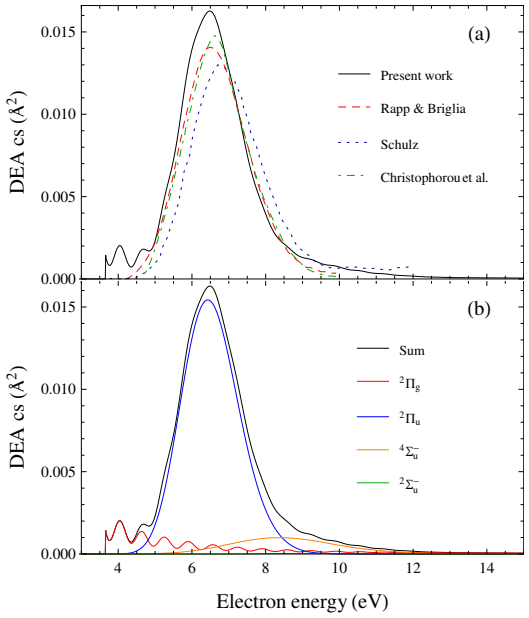

FIG. 2: (Color online) (a) Calculated dissociative electron attachment cross section for $v = 0$ compared with experimental results of Rapp and Briglia [10], Schulz [11] and Christophorou *et al.* [12]. (b) Contributions from the four resonances to the total cross section.

shows a complicated picture with both Π resonances making significant contributions at low energy and important contributions from the Σ resonances at higher energies.

Figure 3 also shows the cross sections for $v = 30$. The increasing trend of the maxima is now inverted. The eigenvalue for this vibrational level [4], in fact, lies above the energy of the $O^-(^2P) + O(^3P)$ asymptotic state (see Fig. 1), so that the DEA process becomes exothermic with a threshold at zero-energy. For this case $R_c > R_e$ so that the exponent ρ in Eq. (5) vanishes ($\Gamma(R > R_c) = 0$) and the magnitude of the cross section is no longer governed by the survival factor. The decreasing trend of the cross section maxima is maintained for $v > 30$.

The corresponding EID cross section from $O_2(X\,^3\Sigma_g^-; v)$ and electron energy ϵ is given by [16]:

$$\sigma_v^{\rm EID}(\epsilon) = \frac{64\pi^5 m^2}{\hbar^4}\int d\epsilon'\frac{k'}{k}\,|\langle\chi_{\epsilon'}(R)|V|\xi(R)\rangle|^2\,, \quad (6)$$

where $\langle\cdots\rangle$ means integration over the internuclear distance R, $\xi(R)$ is the resonant wave function solution of the Eq. (4) and $\chi_{\epsilon'}$ is the continuum wave function of O_2 with energy ϵ' representing the $2O + e^-$ fragments. The continuum energy ϵ' was integrated from O_2 dissociation threshold up to 10 eV.

Figure 4(a) shows the calculated EID cross sections for $v = 0$. Contributions coming from the four O_2^- resonances are shown. Like DEA, the main contribution comes from the $^2\Pi_u$ symmetry, which gives a maximum at 6.93 eV with an absolute value of 0.0072 Å^2, and a

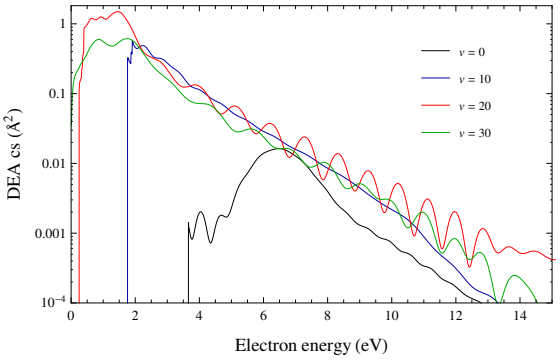

FIG. 3: (Color online) Calculated dissociative electron attachment cross sections for vibrationally excited O_2, for levels $v = 10$, 20 and 30, compared with the ground level $v = 0$. The cross sections include all the four resonant contributions.

significant contribution from the $^4\Sigma_u^-$ at 9.47 eV with a cross section of 0.0026 Å^2. The contribution from the other symmetries is negligible. Figure 4(b) shows the cross sections for excited vibrational levels of oxygen compared with those for the ground level. Cross sections include all four resonance contributions. As expected [18] the EID cross section increases rapidly with vibrational excitation and the threshold moves to lower energy. The cross section for $v = 30$, for example, reaches a value comparable with that of the well-known Shuman-Runge dissociative transitions for the same vibrational level [20], whose dissociative cross sections decrease with increasing the vibrational excitation of the molecule. We note that EID is known to occur efficiently *via* electron impact excitation of O_2 [1, 9]. However the threshold for electronic excitation processes lie significantly higher than those considered here, making them relatively unimportant in low temperature plasmas.

IV. CONCLUSIONS

In conclusion, we present new calculations for dissociative electron attachment for oxygen using *ab initio* potential energy curves and the first calculations for resonant electron-impact dissociation of oxygen. We confirm the dominant contribution of $^2\Pi_u$ symmetry in both processes starting from $v = 0$. Both cross sections however increase rapidly with increase in the vibrational excitation of the molecule and for these vibrationally excited states it is necessary to consider the contributions from all four of the low-lying O_2^- resonance states.

Finally, Fig. 5 compares cross sections for different resonant processes involving electron-$O_2(X\,^3\Sigma_g^-, v)$ scattering: our previous results for $v \rightarrow v + 1$ vibrational-excitation [4], with the present cross sections for DEA and EID for the cases when the O_2 is initially in its vibrational ground state and in its $v = 20$ state. For the $v = 0$ level vibrational excitation is the dominant low-

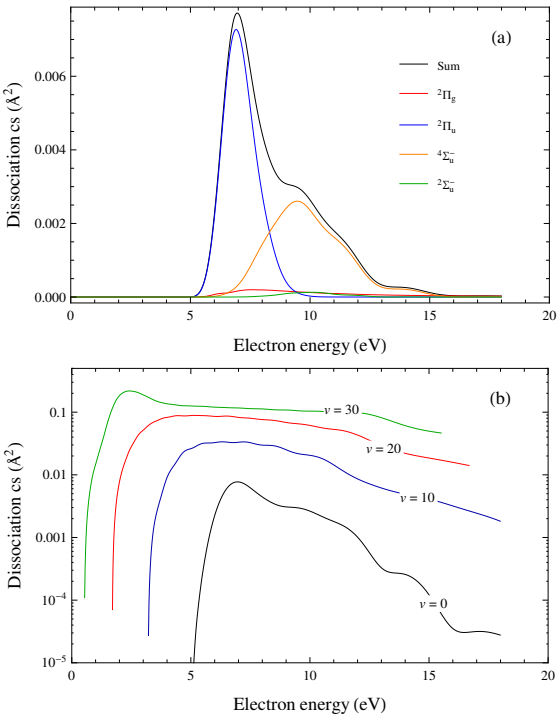

FIG. 4: (Color online) (a) Calculated cross sections for resonant electron impact dissociation of oxygen for $v = 0$. Contributions from the four O_2^- resonances are shown; the black curve is the sum. (b) Dissociating cross sections for vibrationally excited oxygen at $v = 10$, 20 and 30 compared with the results for $v = 0$.

energy process. However for vibrationally excited molecules the DEA increases rapidly and becomes the most important process at low energies. We expect that the inclusion of these results will have important consequences in models of plasmas containing molecular oxygen and, in particular, will lead to a significant increase in O^- ion production in these models.

Recently, we have calculated also the rate coefficients for the processes (1) and (2) as a function of the electronic temperature and for all the vibrational levels. Details of the calculations and results will be reported in [21]. DEA and EID cross sections as a function of electron energy and O_2 vibrational state, along with the corresponding rate coefficients, have been made freely available in the Phys4Entry database [22].

Acknowledgements

The authors are grateful to Prof. M. Capitelli (Università di Bari and IMIP-CNR Bari, Italy) for useful discussion and comments on the manuscript. This work was performed as part of the Phys4Entry project under EU FP7 grant agreement 242311. One of the authors, RC, would like to acknowledge financial support from MIUR-PRIN 2010-11, grant no. 2010ERFKXL.

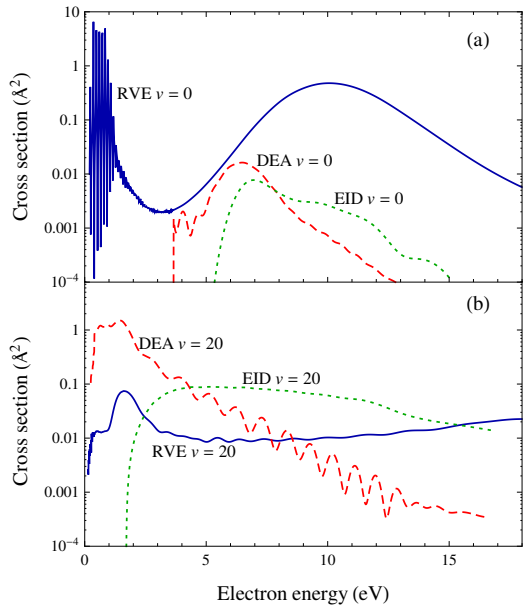

FIG. 5: (Color online) Summary of the cross sections for electron-O_2 collisions: Resonant vibrational excitation for $\Delta v = 1$ transition [4] (solid line), dissociative electron attachment (dashed line) and resonant dissociation by electron impact (dotted line) for (a) $v = 0$ and (b) $v = 20$. The cross sections are the sum over the four O_2^- resonances.

[1] Y. Itikawa, J. Phys. Chem. Ref. Data **38**, 1 (2009).
[2] C. J. Noble, K. Higgins, G. Wöste, P. Duddy, P. G. Burke, P. J. O. Teubner, A. G. Middleton, and M. J. Brunger, Phys. Rev. Lett. **76**, 3534 (1996).
[3] J. Tennyson, Phys. Rep. **491**, 29 (2010).
[4] V. Laporta, R. Celiberto, and J. Tennyson, Plasma Sources Sci. Tech. **22**, 025001 (2013).
[5] H.-J. Werner, P. J. Knowles, G. Knizia, F. R. Manby, M. Schütz, et al., *MOLPRO, version 2012.1, a package of* ab initio *programs* (2012).
[6] J. M. Carr, P. G. Galiatsatos, J. D. Gorfinkiel, A. G. Harvey, M. A. Lysaght, D. Madden, Z. Masin, M. Plummer, and J. Tennyson, Eur. Phys. J. D **66**, 58 (2012).
[7] A. Faure, J. D. Gorfinkiel, L. A. Morgan, and J. Tennyson, Computer Phys. Comms. **144**, 224 (2002).
[8] J. Tennyson, J. Phys. B: At. Mol. Opt. Phys. **29**, 6185 (1996).
[9] J. McConkey, C. Malone, P. Johnson, C. Winstead, V. McKoy, and I. Kanik, Phys. Rep. **466**, 1 (2008).
[10] D. Rapp and D. D. Briglia, J. Chem. Phys. **43**, 1480 (1965).
[11] G. J. Schulz, Phys. Rev. **128**, 178 (1962).
[12] L. G. Christophorou, R. N. Compton, G. S. Hurst, and P. W. Reinhardt, J. Chem. Phys. **43**, 4273 (1965).
[13] T. Jaffke, M. Meinke, R. Hashemi, L. G. Christophorou, and E. Illenberger, Chem. Phys. Lett. **193**, 62 (1992).
[14] P. C. Cosby, J. Chem. Phys. **98**, 9560 (1993).
[15] W. Domcke, Phys. Rep. **208**, 97 (1991).
[16] V. Laporta, D. Little, R. Celiberto, and J. Tennyson, Plasma Sources Sci. Tech. **23**, 065002 (2014).
[17] V. S. Prabhudesai, D. Nandi, and E. Krishnakumar, J. Phys. B: At. Mol. Opt. Phys. **39**, L277 (2006).
[18] D. T. Stibbe and J. Tennyson, New J. Phys. **1**, 2 (1998).
[19] T. F. O'Malley, Phys. Rev. **155**, 59 (1967).
[20] A. Laricchiuta, R. Celiberto, and M. Capitelli, Chem. Phys. Lett. **329**, 526 (2000).
[21] V. Laporta, R. Celiberto, and J. Tennyson, AIP conference proceedings, submitted (2014).
[22] Database of the european union Phys4Entry project, 2012–2014. http://users.ba.cnr.it/imip/cscpal38/phys4entry/database.html